Paper 3

Mass-Standardised Antibody Affinity Maturation to the Spike Protein of SARS-CoV-2 Omicron Variants in a Constant-Exposure Cohort: forgiving Original Antigenic Sin

Philip H. James-Pemberton[1,] Shivali Kohli[2], Aaron C. Westlake[2], Alex Antill[2], Rouslan V. Olkhov[2] and Andrew M. Shaw[1,2*]

[1]Biosciences, University of Exeter, Stocker Road, Exeter, EX4 4QD, UK

[2]Attomarker Ltd, 3 Babbage Way, Exeter Science Park, Exeter, Devon, EX5 2FN, UK

Abstract

Prevalence of SARS-CoV-2 amongst school children in the omicron wave was high leading to a constant exposure of teachers to the virus. A cohort of staff members (n = 28) was recruited from a UK primary school setting. The prevalent variants at the time were Omicron BA.1, BA.4/5 and BA.2: 61% of the cohort reported a lateral-flow-confirmed positive test for SARS-CoV-2 infection in late 2021 or 2022. A mass-standardised quantitative antibody spectrum was measured for both antibody concentration and a new measure of antibody quality; the proportion of antibodies still bound to the epitope at pH 3.2 compared with pH 7.4. The antibody spectrum was measured or IgG to the spike protein for variants Wuhan, Alpha, Beta, Gamma, Delta and Omicron BA.1, BA.2.75, BA.2.12.1, BA.4 and BA.5. The new antibody quality measure shows a mean of 49% with (IQR 32% – 68%). The cohort showed a Universal positive immunity endotype, U(+), of antibodies binding to the spike protein across the variant spectrum with an incidence of 78% (95% CI 60% - 88%) with good antibody concentrations to all ten variants; the incidence drops to 25% (95% CI 13% - 43%) when the affinity spectrum is measured.

Funding – The work was funded by donations from the Exeter University Alumni during the pandemic, by Attomarker Ltd that funded PhD studentship for PHJP at the University of Exeter and Attomarker Ltd directly. Alex Antill was undergraduate at the University of Exeter performing the work as part of their degree.

Declaration of Interest

Prof Shaw is the Founder, CEO and Director of Attomarker Ltd, a spin-out company from his research group.

Related Publications

Paper 1 - Mass-Standardised Quantitative Measurements of the Antibody Levels for SARS-CoV-2 beyond Correlates of Protection and Clearance

Paper 2 - Mass-Standardised Differential Antibody Binding to a Spectrum of SARS-CoV-2 Variant Spike Proteins: Wuhan, Alpha, Beta, Gamma, Delta, Omicron BA.1, BA.4/5, BA.2.75 and BA.2.12.1 variants - Antibody Immunity Endotypes

Paper 3 – this paper - Mass-Standardised Antibody Affinity Maturation to the Spike Protein of SARS-CoV-2 Omicron Variants in a Teachers Cohort: forgiving Original Antigenic Sin

Paper 4 - Diagnostic Classification for Long Covid Patients identifying Persistent Virus and Hyperimmune Pathophysiologies leading to a Test-and-Treat Protocol

Introduction

School staff members are uniquely exposed to transient infections in children when in enclosed, poorly ventilated environments, including during the SARS-CoV-2 pandemic[1]. A retrospective test-and-trace study from Italy[2] has shown that, of the school students in the age range 6 -10 years, 50% (95% CI, 39% - 60 %) tested positive and were asymptomatic carriers and 21.4% (95% CI 14% – 31%) had symptomatic infections for SARS CoV-2. Similarly, studies in the UK following the release of school teaching restrictions showed a surge in student infections during the period August to October 2021[3] with household clusters adding to transmissions in parents, particularly from children aged 5-15. Other studies counter with findings that school children in the pandemic[4] in the age range 5–11 years old did not have a prevalence of infection greater than the local working population, although the prevalence of asymptomatic carriers was not reported.

A teachers' cohort is a constant-exposure cohort addressing directly the concepts of immunity imprinting and original antigenic sin [5-7] with continual challenges evolving the antibody epitope selection and the T cell response. In a previous study[8], we observed antibody immunity endotypes to a spectrum of variants: Wuhan, Alpha, Beta, Gamma, Delta and Omicron variants: BA.1, BA.4, BA.5, BA.2.75 and BA.2.12.1. A universal endotype showed antibody concentrations to all variants was present in 75% of the cohorts tested. The universal protection is consistent with raising antibodies to conserved epitopes, such as the hinge region required for the Spike protein to transition from pre-fusion to fusion state[9]. Meanwhile, immunity endotypes of the remaining 25% show poor antibody production or drop-outs to one or more of the variants, having made antibodies to epitopes that are not present in all variants, potentially leading to a risk of post-viral sequalae[10-12].

Immunity endotypes were previously explored for the concentration of antibodies against variant spike proteins[8] but affinity of the antibody-antigen interactions is also an important and potentially evolving immunity endotype and critical to the clone selection process[13]. Measurement of antibody affinity (or avidity) requires the association and dissociation rates of the paratope-epitopes complex to be accurately measured, and for stable complexes this corresponds to a half-life of several hours[14]. A high-affinity antibody in an immune response suggests the clearance proves needs a stable complex. Further, affinity studies are usually performed at pH 7 which is poor mimic of the mucosal environment where the pH may be more acidic, pH 5.5. Here, we have explored a new method of assessing the stability of the

paratope-epitope complex by measuring a ratio between antibody-antigen binding responses at two different pH values: pH 3.2 and pH 7.4. Titration of the paratope-epitope complex shows that affinity (or avidity) could be pH dependent and so environment dependent. The critical parameter in forming a high-quality antibody response is the antibody-antigen complex lifetime in all environments which controls the timescales on which an antibody-mediated response such as endocytosis or complement action takes place leading to a sterilising event and removal of the virus.

In this paper, we report a prospective cohort study on 28 staff members in a primary school setting with samples taken 13th July 2022. The local prevalent Omicron variants at the time of sampling were BA.4 and BA.5, whilst BA.1.1 and BA.2 were prevalent in the preceding six months. Demographic data was collected alongside vaccination histories and lateral flow confirmations of any recent infections. A COVID antibody immunity test was performed for nucleocapsid, Spike (Wuhan), Spike Omicron BA.1 and receptor binding domain. Further, concentration and pH-dependent affinity profiles were collected for the spike proteins of the variants Wuhan, Alpha, Beta, Gamma, Delta, as well as Omicron strains BA.1, BA.2.75, BA.2.12.1, BA.4 and BA.5. The full 20-dimensional profile of concentration and pH-dependent affinity for 10 variants for each adult tested in the school was interpreted in the constant-exposure cohort context and optimisation of the high-avidity antibody response.

Materials and Methods

Materials

Materials used throughout the course of the experiments were used as supplied by the manufacturer, without further purification. Sigma-Aldrich supplied phosphate buffered saline (PBS) in tablet form (Sigma, P4417), phosphoric acid solution (85 ± 1 wt. % in water, Sigma, 345245) and Tween 20 (Sigma, P1379). Glycine (analytical grade, G/0800/48) was provided by Fisher Scientific. Assay running and dilution buffer was PBS with 0.005 v/v % Tween 20 and the regeneration buffer was 0.1 M phosphoric acid with 0.02 M glycine solution in deionized water.

A recombinant human antibody to the spike protein S2 subdomain, a chimeric monoclonal antibody (SinoBiological, 40590-D001, Lot HA14AP2901) was used as a calibrant. The antibody was raised against recombinant SARS-CoV-2 / 2019-nCoV Spike S2 ECD protein (SinoBiological, 40590-V08B). This was selected as it could bind to all nine Spike protein variants used herein.

NISTmAb, a recombinant humanized IgG1κ with a known sequence[15] specific to the respiratory syncytial virus protein F (RSVF)[16], was from National Institute of Standards and Technology (RM8671). The detection mixture consisted of a 200-fold dilution of IG8044 R2 from Randox in assay running buffer. The Spike Variant sensor chips were printed as detailed elsewhere[17]. The Omicron sub-variant sensor chips were printed with recombinant human serum albumin from Sigma-Aldrich (A9731), protein A/G from ThermoFisher (21186), and five SARS-CoV-2 Spike Protein variants for the Wuhan, Omicron BA.1, BA.4, BA.5, BA.2.75 and BA.2.12.1 strains from SinoBiological and BA.2.75 strain from Acro Biosystems as detailed in Table S1.

Methods

Biophotonic Multiplexed Immuno-kinetic assay

The multiplexed biophotonic array platform technology has been described in detail elsewhere[8,17-20] and has a CE mark to perform the Attomarker COVID Antibody Immunity and a UKCA mark for the Covid Antibody Spectrum Test. Briefly, the technology is a localised particle plasmon gold sensor which scatters light proportional to the mass of material (formally refractive index) near to the gold nanoparticle surface in the plasmon field. The gold nanoparticles are printed into an array of 170 spots which are then individually functionalised with the protein required. The SARS-CoV-2 antibody targets within the CE marked COVID Antibody immunity Test are nucleocapsid, receptor binding domain, Wuhan spike protein and Omicron spike protein. The inflammation marker C-reactive protein is also measured. The assay consists of a capture step, a detection step and a regeneration step with intervening wash steps. High and low controls are used to calibrate the sensor response and are repeated at regular intervals to ensure quality control[15] during the day.

Two further arrays were fabricated. One containing Spike proteins from SARS-CoV-2 variants, as detailed elsewhere[8], alongside a new array containing the Omicron sub-variants as listed in Table S1. The integrity of the protein samples on the surface was tested using an anti-S2 antibody (40590-D001), chosen for calibration as the corresponding epitope is present on all variants. The concentration of the antibody was calibrated against the NIST antibody RM8671, NISTmAb, a recombinant humanized IgG1κ with a known sequence[15] to assure monomeric purity of the antibody. High-control and low-control samples were made using the 40590-D001 antibody and these controls were then used to quantify results from human

samples in units of mg/L. Thus, the assay response is presented as a concentration of an antibody equivalent in its binding properties to the 40590-D001 control antibody. An assay common to each sensor chip was performed using the S (Wuhan) channel, with each array carrying an identical protein. There was high correlation between S channel performance on the two array types (m, c >0.92) and so the results were treated as aligned, Table S2 and Figure S2.

An endotype classification has been derived for the spike protein variant[8] and The average of all thresholds is 1.8 mg/L (the Limit of Detection (LoD) of the technique is 0.2 mg/L) and a universal positive endotype, U(+), has the antibody concentrations for all variants above the 1.8 mg/L threshold. A single drop-out has an antibody concentration for one variant below the threshold, *e.g.* β(-), double drop-out, two variants α(−)β(-) *etc*., for all variants and these are all labelled U(±); one or more variant antibody concentrations <1.8 mg/L. A full correlation analysis for all combinations of responses was also performed from which the correlation coefficients and lines of best fit were derived. A new measure of antibody affinity has been derived comparing the antibody binding on the surface of the target antigen after a 30 s wash step at either physiological serum pH 7.4 or pH 3.2. The lower pH of 3.2 results in some dissociation of the paratope-epitope complex leading to an effective reduction of the measured antibody concentration; a measurement of the antibodies that remain strongly bound at pH 3.2 – a high-affinity concentration. A full dissociation occurs at pH 1.9; the pH used at the longer regeneration step. The antibody profile is parameterised by the total antibody concentration (AC), the high-Quality antibody concentration (HQ) and the percentage of high-quality antibodies (HQ% = HQ/AC ×100). The cohort was used to determine reference ranges for these two new immunological measures. The HQ% from the cohort was used to estimate the HQ threshold of a sterilising serum, scaling the AC threshold derived elsewhere[17].

Patient Cohort

The staff members were recruited from a primary school setting and took the CE marked Attomarker Antibody Immunity Test after giving informed consent with a registered healthcare professional for the use of their residual blood samples to be used in aiding understanding of the pandemic. The venous blood samples were analysed on site within 7 minutes, and the results subsequently provided to the patients. The residual vacutainer blood

was transported back to the laboratory and centrifuged at 1300 rpm for 10 minutes to separate the blood constituents. The serum was collected and subsequently used for variant profile screening.

Ethical Approval

The use of the Attomarker clinical samples was approved by the Bioscience Research Ethics Committee, University of Exeter.

Results

The teachers cohort recruited from the school was 86% female and 14% male: 68% had an initial AstraZeneca (AZ) two-vaccination dose, 25% Pfizer, 4% Moderna and 4% undeclared, Table 1 (and Table S4). Seven teachers in the cohort, or 25 % (95% CI 13% - 43%), were un-boosted. Each teacher had a full concentration and pH-dependent affinity profile assessment for each of the ten spike proteins. A pH-dependent affinity titration for a teacher is shown in Figure S3 for nucleocapsid, Spike protein, Omicron Spike Protein and receptor binding domain. Each of the paratope-epitope titrations show a fall in binding of approximately 50% at pH 3.2, which was selected as the differentiating pH for the HQ and HQ%, to give a good dynamic range. The defining reference range for these new parameters is derived by assuming HQ% is a clone selection property and constant for all variants. The mean and interquartile range (IQR) for HQ% was derived from Wuhan, BA.1, BA2.12.1 BA.2.75. BA.4 and BA.5 to give HQ% is 49% (IQR 32% - 68%), Table S5.

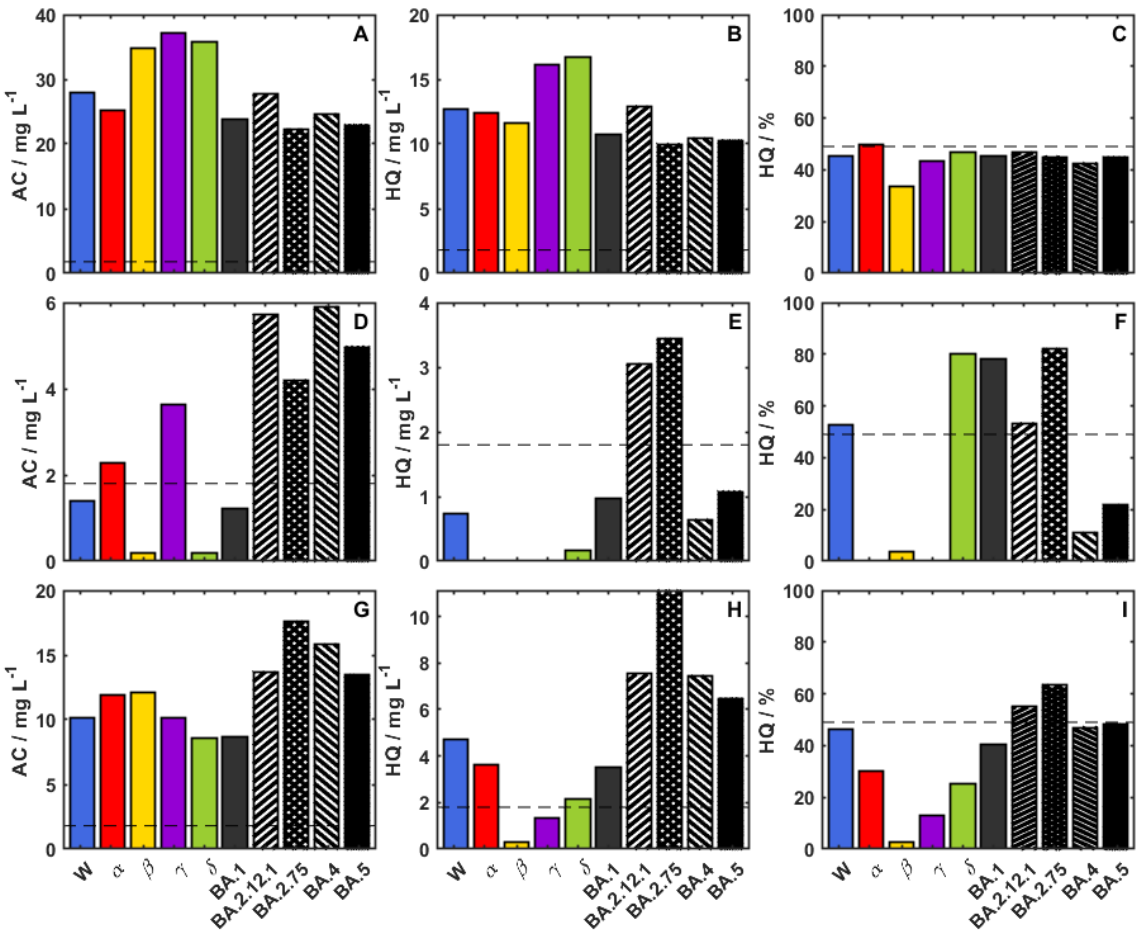

Figure 1 Three patients are presented , one per row, showing 10-variant antibody spectra: (A,B,C) is the profile of one patient showing antibody concentration (AC), High-quality antibodies (HQ) and the HQ as percentage of AC, HQ% - this

sample is a U(+) endotype;. Patient 2 (D,E,F) shows U(-) endotype for β(-) and δ(-)for AC but falling)only BA.2.12.1 and BA.2.75 variants; and Patient 3 (G,H,I) showing a U(+) for AC but low concentrations for HQ indicating poor antibody quality except for BA2.12.1 and BA.2.75, the circulating variants. and Patient 3 (G,H,I) all show drop-out endotypes but good quality antibodies to the circulating variants at the time. The dotted line for the AC antibodies is set at the sterilising serum threshold; the dotted line for HQ is set at 49% of the sterilising threshold and the dotted line for HQ% is set at 49%.

The mean HQ% is used to covert the sterilising serum threshold total (recovering patient cohort accuracy study[17]) to derive a threshold for the sterilising serum HQ. Both thresholds are shown for some patent antibody spectra, Figure 1. The teacher cohort has a confirmed infection incidence in the preceding six months of 61% (95% CI 42% -76%) and a U(+) incidence of 78% (95% CI 60% - 88%) consistent with the incidence observed in our previous study[8], shown in Figure 1(A). Of the remaining six teachers, five showed a Delta drop-out endotype either alone or in combination with Beta variant: the two Beta variant drop-out endotypes were associated with a Pfizer vaccination history similar to previous observations[8]. The U(+) incidence in the cohort changes for the HQ and HQ% parameters as seen for Patient 3 Figure 1 (G, H, I) where AC concentration for each variant looks strongly U(+) but HQ antibodies are much greater in the Omicron variants with an average of 49%. The total Universal Immunity endotype, U(+), incidence falls by a third to 25% (95% CI 13% - 43%). The drop-out variants (*n*=18 or 64% (95% CI 46% - 79%)) are exclusively early variant dropouts: none are Omicron variant, Table 1.

Table 1 Cohort demographics including vaccination profile, infection history and endotype classification for concentration and high-affinity concentration (AstraZeneca (AZ), Undeclared (U), U(+) is the universal endotype, variant dropouts α,β,γ,δ,ο and unclassified (UC)) (Sample IDs are not known to the patient)

Sample ID	Interval since recent positive test	Vaccine	Booster	Number of doses	Quantity Endotype (<1.8 mg/L)	High Quality Endotype (<0.9 mg/L)	High Quality Endotype (<49%)
C104	< 4 months	AZ	U	3	U(+)	U(+)	6-
C105		Pfizer	Pfizer	3	Wβδ (-)	5-	7-
C106	< 4 months	Pfizer	Pfizer	3	U(+)	3-	9-
C107	< 5 months	Pfizer		2	W,BA.1,βδ (-)	6-	3-
C108	< 1 month	AZ	Pfizer	3	U(+)	1-	6-
C109	< 5 months	AZ	Moderna	3	U(+)	U(+)	0-
C110	< 6 months	Pfizer		2	U(+)	3-	6-
C111	< 1 month	AZ	Moderna	3	U(+)	4-	10-
C112		AZ	Moderna	3	U(+)	1-	5-
C113	< 1 month	U	U	3	U(+)	U(+)	6-
C114	< 4 months	Pfizer	Pfizer	3	βδ (-)	5-	4-

C115	< 5 months	AZ	Pfizer	3	U(+)	U(+)	4-
C116	< 3 months	AZ	U	2	U(+)	1-	8-
C117	< 2 months	AZ	Moderna	3	U(+)	U(+)	8-
C118		Moderna	Moderna	3	U(+)	2-	9-
C119		AZ		2	βδ (-)	5-	7-
C120	< 3 months	Pfizer	Pfizer	3	U(+)	3-	7-
C121		AZ	Moderna	3	U(+)	U(+)	9-
C122	< 3 months	AZ		2	U(+)	1-	10-
C123		AZ	Pfizer	3	U(+)	4-	9-
C124		AZ	Pfizer	3	δ (-)	4-	7-
C125		Pfizer		2	U(+)	U(+)	3-
C126	< 1 month	AZ	Pfizer	3	U(+)	1-	2-
C127	< 1 month	AZ	Moderna	3	U(+)	U(+)	8-
C128	< 4 months	AZ	Moderna	3	U(+)	1-	8-
C129		AZ	Moderna	3	U(+)	U(+)	9-
C130	< 8 months	AZ	Pfizer	3	δ BA.2.75(-)	6-	5-
C131		AZ		2	U(+)	U(+)	5-

The cohort bee-swarm box-plots shown in Figure 2 show median concentrations for all variants to be equivalent (Table S5), but with significantly lower median pH-dependent affinity values (Wilcoxon: Wuhan *vs* Beta $P = 6.1x10^{-8}$, Wuhan *vs* Gamma $P = 5.3x10^{-6}$). The dynamic range of the HQ% is 10% – 100% and shows discrimination, potentially with bimodal distributions, across the teacher cohort in favour of Omicron variants.

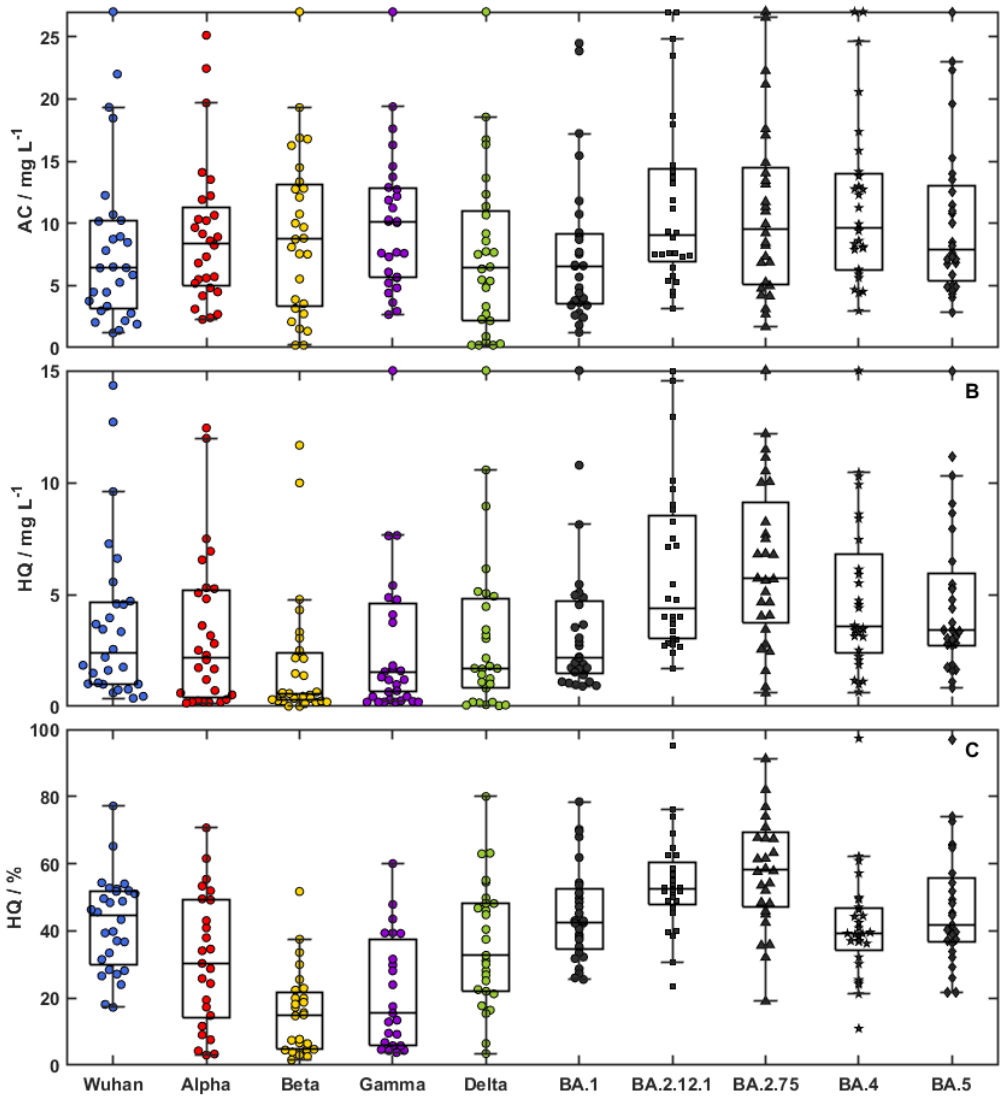

Figure 2 Bee-swarm plot for the Cohort Profiles: (top panel) concentration, (middle panel) high-affinity concentration and Antibody Efficiency (lower panel)

Discussion

The teacher cohort is uniquely exposed in the school setting to children, especially of younger age, that are either asymptomatic carriers or symptomatic cases[2,3] in the COVID pandemic. The repeated, evolving exposure is the in the 'new-normal' where repeated waves of infection lead to a high virus prevalence and infection. Schools have been identified[21] as foci of the pandemic although the children themselves may not be vulnerable to infection, leading to difficult discussions about child vaccination[22]. Countries have differed approaches despite WHO recommendations[23]. The effect of re-opening schools in the UK showed significant increase in infection rates amongst school children[21]. The teachers and parents of school children represent one of the critical immunity perimeters of the pandemic with consequent implications for workforce sickness and impact on economic activity.

The constant-exposure teachers' cohort, whether unvaccinated, vaccinated or boosted, are exposed repeatedly to the prevalent circulating virus to which there is a significantly refined immunity response. Immunity Imprinting has been reported for SARS-CoV-2 vaccination[24] and we have reported immunity endotypes for antibody concentration against a spectrum of variant spike proteins[8] suggesting that initial exposure to a virus or vaccine may imprint a remembered immune response. Antibody quality or antibody affinity maturation has been reported for SARS-CoV-2 immunity[25,26] with mechanisms of maturation proposed in the germinal centre B cell response[27,28] critical to the adaptive immunity response[29]. Sustained antigen availability has also pointed to non-standard vaccination strategies to optimise the adaptive response[30,31]. The teacher cohort is therefore an ideal setting for the observation of antibody immunity imprinting and consequence maturation: the forgiveness of original antigenic sin.

There is a spectrum of immunity in the teacher cohort derived from vaccination as well as boosted staff (four of whom reported sickness and had time off work), Table 1. The incidence of lateral-flow-test-confirmed infection in the preceding six months was 63% suggesting exposure to BA.1.159, BA.4/5 and BA.2, Figure S1. The antibody concentration profile across the spectrum of spike proteins showed the cohort incidence of U(+) was 75% and reflects previous measurements indicating that many had moderate-high antibody levels to all variants, potentially from targeting a universal epitope most likely located on the hinge region of the protein[8]. However, the new measure of antibody quality, pH-dependent affinity, shows significant variation across variants. The Wuhan antibodies generated by the boosted vaccination, and so renewed exposure to the antigen, showed affinity similar to the prevailing variants but was significantly worse for Alpha, Beta and Gamma (Kolmogorov-Smirnov test P values: Alpha=0.016, Beta=4.1×10^{-8}, Gamma=1.84×10^{-5}, Delta=0.28, BA.2.12.1=0.016, BA.2.75=0.0023, BA.4=0.47, BA.5=0.91, BA.1=0.91 *vs* Wuhan). Thus, the U(+) endotype incidence drops to 25%. Figure 1 (A, B, C), shows access to the universal epitope, fully affinity-matured to all variants following vaccine exposure, a highly efficient adaptive response. However, some U(+) endotypes with promising antibody concentration profiles, Figure 1 (G, H, I), do not have antibodies matured against Beta or Gamma variants, leading to lower high-affinity antibody concentration and therefore lower vaccine efficiency against these particular variants. The cohort distributions show a significant antibody maturation and consequent vaccine efficacy towards the Omicron sub-variants (High-Affinity Concentration data Kolmogorov-Smirnov test P values: Alpha=0.47, Beta=0.0023, Gamma=0.15, Delta=0.47, BA.2.12.1=0.0062, BA.2.75=0.016, BA.4/5=0.15, BA.1=0.91 *vs* Wuhan), with maximum efficiency for the variants BA.2.12.1 and BA.2.75, both descending from the widely circulated BA.2 lineage. There were no Omicron endotype dropouts in contrast to the vaccination cohort not in continuous exposure, with an incidence of 7% (95% CI 2% - 19%)[8].

The new measure of pH-dependent affinity, HQ%, has a mean of 49% with (IQR 32% – 68%) is an easy way to assess the dissociation constant of the epitope-paratope complex which typically has a half-life 0.5 – 2 hours. The pH-dependent affinity is used routinely in the elution of antibodies at pH 2.5-3.0 during affinity chromatography[32] suggesting the binding complex can be titrated as shown in Figure S3 for the proteins N, RBD, S(Wuhan), and S(Omicron) although the variation is complex and highly protein dependent. A linear correlation has been shown with the complex half-life and Affinity constant, K_D (pM) shown in Figures S4 and S5. Further, the physiological importance of lower pH is also relevant to the nasal mucosa[33], which at pH 5.5 – 6.5, is significantly lower than the pH of the serum and the buffers used for conventional affinity measurements. A nasal mucosal protection mechanism, pH 5, would require antibody complexes to be sufficiently numerous and stable to prevent attachment to the angiotensin-converting-enzyme-2 receptor, a parameter described here as the high-affinity concentration.

Conclusions

The immunity profile for staff in the constant-exposure cohort has been characterised in 30 dimensions: 10 variant spike proteins, total antibody concentration, AC, the high-quality antibody concertation, HQ, and the percentage of high-quality antibodies, HQ%, which are now all measures of a sterilising serum for the clearance of different variants of the SARS -CoV-2 virus. Technique independent thresholds and references ranges have been set of these serum characteristics. The patient antibody spectra show significant antibody maturation to all SARS-CoV-2 variant spike proteins, notably to the prevalent Omicron variants. Approximately, 25% of the cohort have full, pan-variant protection whereas the remainder have higher-quality antibodies focused on the preceding wave variants. A smart-boosting programme focused on high-transmission groups, such as teachers and parents/guardians of school-age children, could significantly reduce the risk of high infection levels within the population during each wave, as the pandemic transitions to endemic. Furthermore, extensive and readily measured immunity profiles may highlight specific endotype vulnerability to infection, and provide insight into long COVID complications.

Acknowledgements

Professor Shaw's Research Group at Exeter University and Attomarker would like to thank the schoolteachers and staff who participated in this research project. The authors would like to thank Dr

Jonathan Snicker for their guidance on the potential strategic and policy implications of the scientific findings.

Supplementary Data

Figures

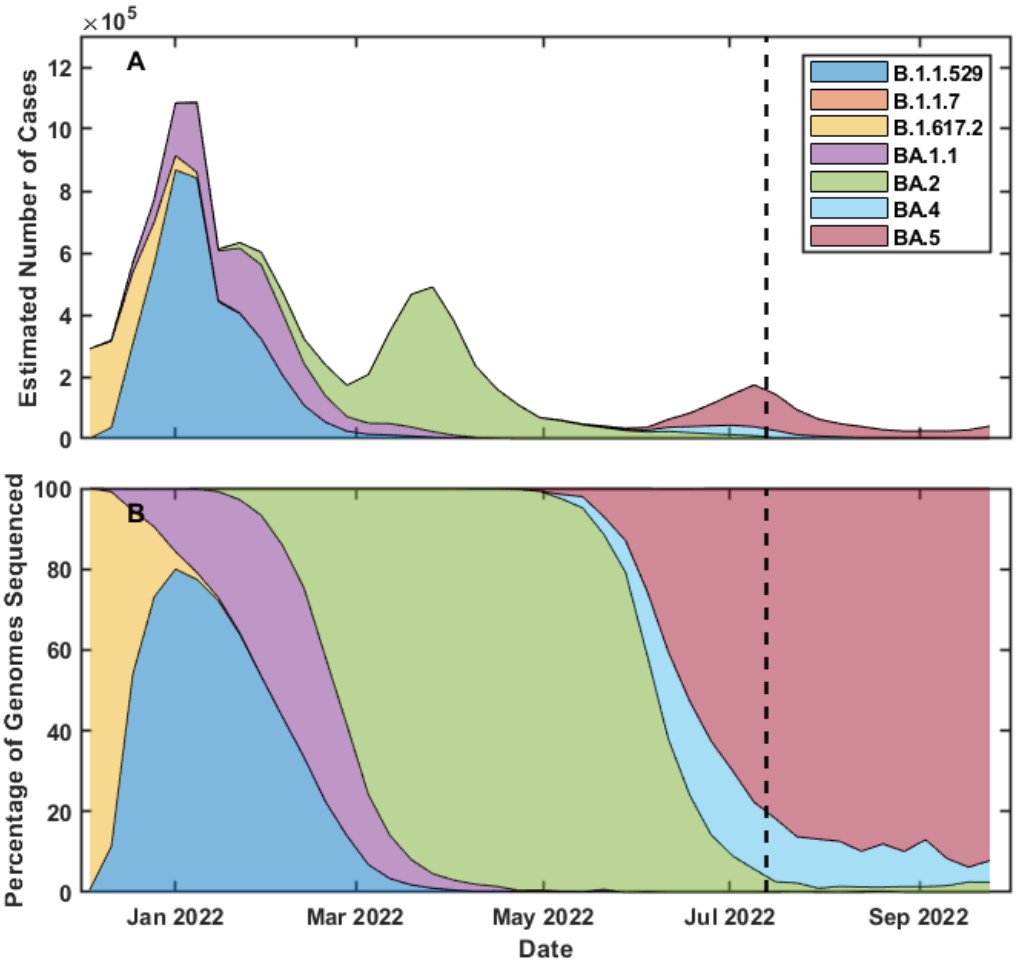

Figure S1 Prevalent SARS-CoV-2 variants preceding the cohort screen and the date of the cohort testing – shown using the black-dash line. Data is taken from the Wellcome Sanger Institute [34]. – this may need to be updated.

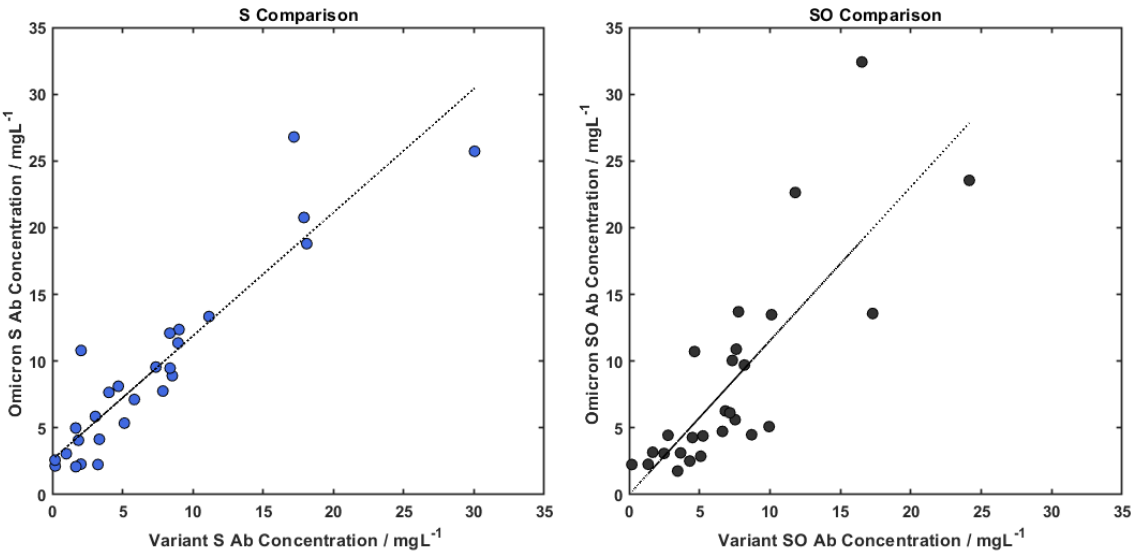

Figure S2. Correlation of Spike and Omicron Spike channels on the Variant and Omicron Sub-variant Arrays. – R^2 values in the caption or the slopes and intercept.

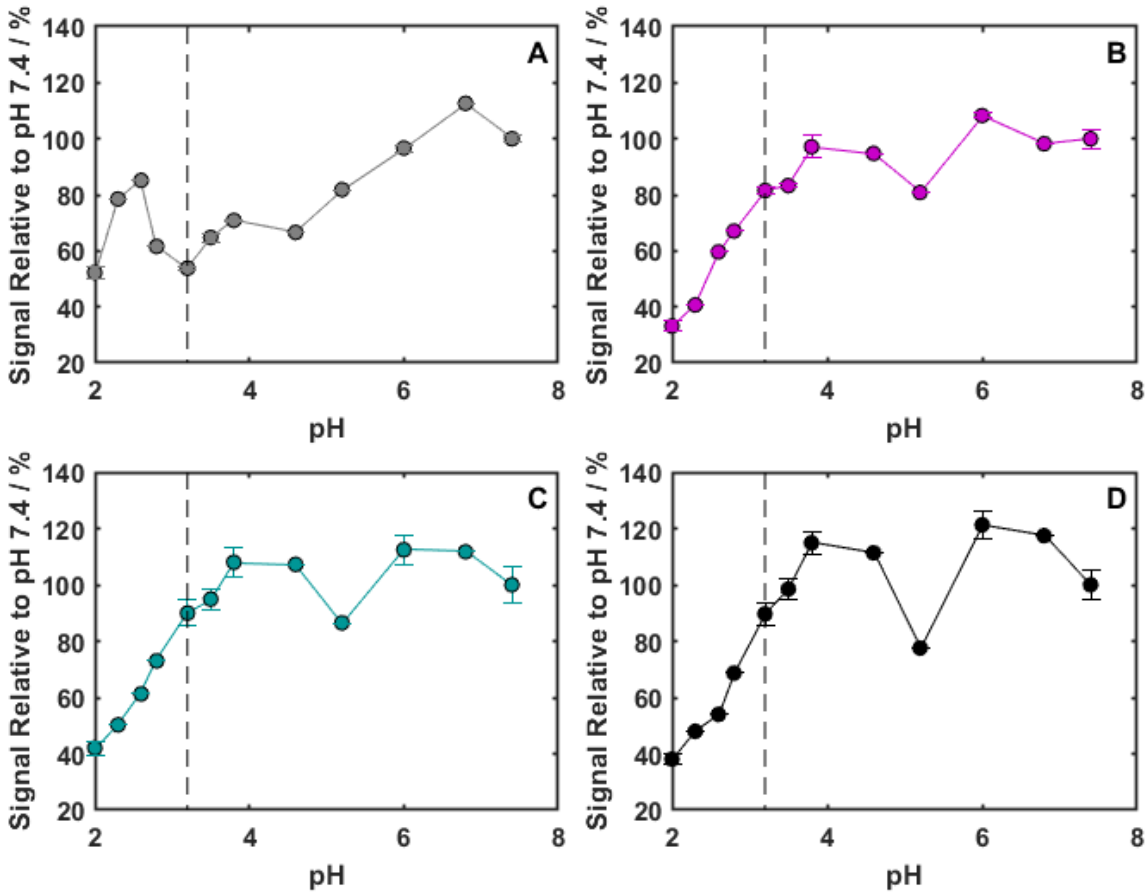

Figure S3 The change in concentration of the antibody assay with pH of an intermediate wash step. Protein Channels shown are the SARS-CoV-2 viral proteins: A) Nucleocapsid, B) RBD, C) S (Wuhan) and D) S (Omicron BA.1). Error bars show 1 SD. The vertical dotted line is drawn at pH 3.2.

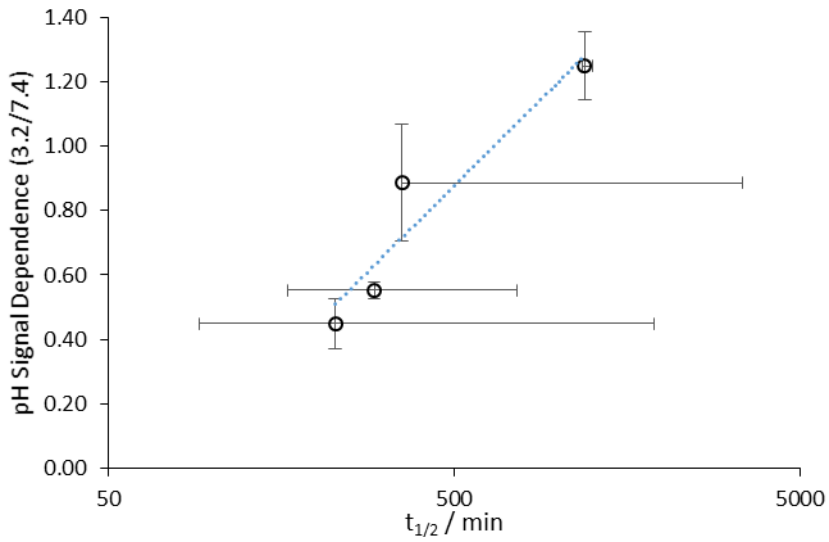

Figure S4 Plot of antibody-antigen half-life at pH 7.4 vs the pH dependence of the complex stability. Error bars show 1SD. The half-life was measured for four commercially sourced antibodies by recording the antibody dissociation over 20-30 minutes and fitting the data produced to a Langmuirian model. The pH dependence was determined by a sandwich assay with an intermediate wash step of 30s (between capture and detection) of varying pH.[ZHU1076 (Sigma-Aldrich), 40590-D001, 40590-T62 (Sinobiological), antiS2 1034617 (Biotechne)]. – this is going to hurt us – we need to think about it.

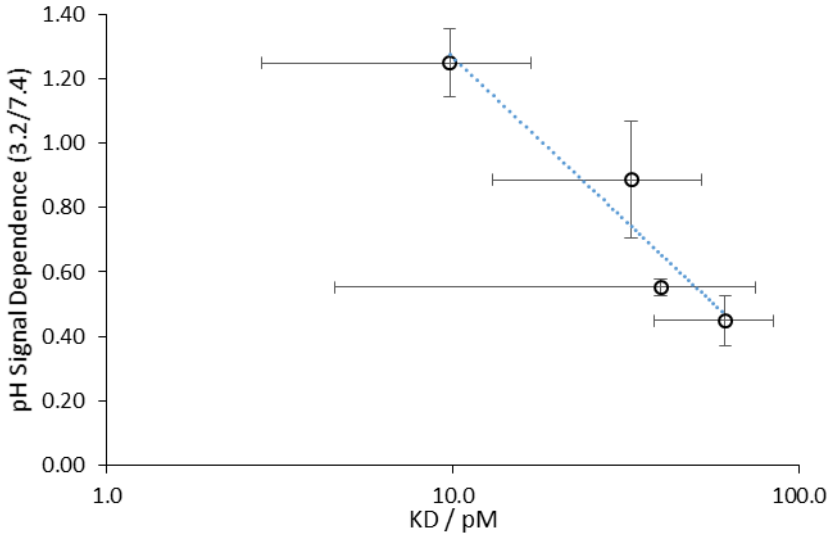

Figure S5 Plot of antibody K_D at pH 7.4 against the pH dependence of the complex stability. Error bars show 1 SD.

Tables

Table S1. The Spike proteins used to fabricate the Omicron Sub-variant test arrays.

Protein	Supplier	Cat #	Lot # (s)	Type	Cell Line	Tag	AA Length	Mutations
Wuhan	Sinobiological	40589-V08B1	MF16JU1612	Monomer	Baculovirus-Insect	C-term polyhistidine	1209	-
BA.1	Sinobiological	40589-V08H26	LC16JA1515	Trimer	HEK293	C-term polyhistidine	1228	A67V, HV69-70 deletion, T95I, G142D, VYY143-145 deletion, N211 deletion, L212I, ins214EPE, G339D, S371L, S373P, S375F, K417N, N440K, G446S, S477N, T478K, E484A, Q493R, G496S, Q498R, N501Y, Y505H, T547K, D614G, H655Y, N679K, P681H, N764K, D796Y, F817P, N856K, A892P, A899P, A942P, Q954H, N969K, L981F, K986P, V987P and furin cleavage site mutants
BA.2.12.1	Sinobiological	40589-V08H34	MB16JU1681	Trimer	HEK293	C-term polyhistidine	1228	T19I, L24S, del25-27, G142D, V213G, G339D, S371F, S373P, S375F, T376A, D405N, R408S, K417N, N440K, L452Q, S477N, T478K, E484A, Q493R, Q498R, N501Y, Y505H, D614G, H655Y, N679K, P681H, S704L, N764K, D796Y, A892P,

								A899P, A942P, Q954H, N969K, K986P, V987P and furin cleavage site mutants
BA.2.75	Acro Biosystems	SPN-C522f	6764A-227DF1-146	Trimer	HEK293	C-term polyhistidine	1197	.T19I, LPP24-26del, A27S, G142D, K147E, W152R, F157L, I210V, V213G, G257S, G339H, S371F, S373P, S375F, T376A, D405N, R408S, K417N, N440K, G446S, N460K, S477N, T478K, E484A, Q498R, N501Y, Y505H, D614G, H655Y, N679K, P681H, N764K, D796Y, Q954H, N969K, R683A, R685A, F817P, A892P, A899P, A942P, K986P, V987P. Proline substitutions (F817P, A892P, A899P, A942P, K986P, V987P) and alanine substitutions (R683A and R685A) are introduced to stabilize the trimeric prefusion state of SARS-CoV-2 S protein and abolish the furin cleavage site, respectively.
BA.4	Sinobiological	40589-V08H32	MB16JU1382	Trimer	HEK293	C-term polyhistidine	1226	F817P, A892P, A899P, A942P, K986P, V987P, T19I, L24del, P25del, P26del, A27S, H69del,

								V70del, G142D, V213G, G339D, S371F, S373P, S375F, T376A, D405N, R408S, K417N, N440K, L452R, S477N, T478K, E484A, F486V, Q498R, N501Y, Y505H, D614G, H655Y, N679K, P681H, N764K, D796Y, Q954H, N969K and furin cleavage site mutants
BA.5	Sinobiological	40589-V08H33	MB16JU1383	Trimer	HEK293	C-term polyhistidine	1226	F817P, A892P, A899P, A942P, K986P, V987P, T19I, L24del, P25del, P26del, A27S, H69del, V70del, G142D, V213G, G339D, S371F, S373P, S375F, T376A, D405N, K417N, N440K, L452R, S477N, T478K, E484A, F486V, Q498R, N501Y, Y505H, D614G, N679K, P681H, N764K, D796Y, Q954H, N969K and furin cleavage site mutants
Alpha	**Sinobiological**	**40589-V08B6**	**LC15MC0903**	**Monomer**	**Baculovirus-Insect**	**C-term polyhistidine**	**1206**	**HV69-70 deletion, Y144 deletion, N501Y, A570D, D614G, P681H, T716I, S982A, D1118H**
Beta	Sinobiological	40589-V08B7	LC15MY2607	Monomer	Baculovirus-Insect	C-term polyhistidine	1206	L18F, D80A, D215G,

								LAL242-244 deletion, R246I, K417N, E484K, N501Y, D614G, A701V
Gamma	Sinobiological	40589-V08B8	LC15JU0209	Monomer	Baculovirus-Insect	C-term polyhistidine	1209	L18F, T20N, P26S, D138Y, R190S, K417T, E484K, N501Y, D614G, H655Y, T1027I
Delta	Sinobiological	40589-V08B16	LC15OC2012	Monomer	Baculovirus-Insect	C-term polyhistidine	1207	T19R, G142D, E156G, HR157-158 deletion, L452R, T478K, D614G, P681R, D950N
Omicron	Sinobiological	40589-V08B33	MF15DE2961	Monomer	Baculovirus-Insect	C-term polyhistidine	1206	A67V, HV69-70del, T95I, G142D, VYY143-145del, N211del, L212I, ins214EPE, G339D, S371L, S373P, S375F, K417N, N440K, G446S, S477N, T478K, E484A, Q493R, G496S, Q498R,

					N501Y, Y505H, T547K, D614G, H655Y, N679K, P681H, N764K, D796Y, N856K, Q954H, N969K, L981F

Table S2. Gradient (m), intercept (c) and R^2 values for the correlation of similar channels on the Spike Variant Array and the Spike Omicron Array.

Protein Pair x/y	**Slope**	**Intercept**	**R^2**
S (monomer)/S (monomer)	0.93	2.6	0.92
SO (monomer) /SO (trimer)	1.15	0.0	0.81

Table S4. Antibodies used for production of $t_{1/2}$ to k_d plot.

Ab	**Immunogen**	**SKU**	**Batch**	**Manufacturer**	**Type**
Clone hu2B3E5 ZooMAb	Recombinant S fragment from SARS-CoV	ZHU1076	Q3506110	Sigma Aldrich	Mouse/Human recombinant monoclonal
Spike S2 Antibody	Recombinant SARS-CoV-2 Spike S2 ECD (#40590-V08B)	40590-D001	HA14AP2901	Sinobiological	Rabbit/Human recombinant monoclonal
anti S2 1034617	Recombinant SARS-CoV2	MAB10557-100	CNEF0121021	Biotechne	Mouse Monoclonal

Spike S2 Antibody	Spike S2 Subunit Recombinant SARS-CoV-2 Spike S2 ECD (#40590-V08B)	40590-T62	HD15JU0103	Sinobiological	Rabbit polyclonal

Table S5 Ranges for the AC, HQ and HQ% derived from the cohort showing median, d Lower Quartile (LQ) and Upper Quartile (UQ: HQ% W, BA.1, BA2.12.1 BA.2.75. BA.4 and BA.5

	Wuhan	**Alpha**	**Beta**	**Gamma**	**Delta**	**BA.1**	**BA.2.12.1**	**BA.2.75**	**BA.4**	**BA.5**
AC / mg L^{-1}										
LQ	3.2	5.3	3.7	5.7	2.5	3.5	6.9	5.1	6.2	5.4
Median	6.4	8.6	8.8	10.2	6.5	6.6	8.8	9.9	9.9	8.2
UQ	10.2	11.3	13.1	12.8	11.0	9.1	14.4	14.5	14.0	13.0
HQ / mg L^{-1}										
LQ	1.0	0.6	0.3	0.4	0.9	1.5	3.2	3.7	2.8	2.7
Median	2.6	2.3	0.6	1.2	1.7	2.2	4.8	5.7	3.6	3.4
LQ	1.0	0.6	0.3	0.4	0.9	1.5	3.2	3.7	2.8	2.7
HQ / %										
LQ	32	10	5	5	22	34	49	47	37	37
Median	44	27	15	11	32	43	53	58	39	42
UQ	51	43	20	32	48	54	63	68	47	54
Reference Range Mean and IQR										
49% (32% – 68%)										

Table S2 Additional cohort demographics.

Age	16-24	25-34	35-44	45-54	55-64	65-74	75+
%	4	14	14	21	32	11	4
Initial 2 Dose Vaccine	**AZ**	**Pfizer**	**Moderna**	**Unknown**			
%	68	25	4	4			

Table S3 Channels grouped according to time. Early = all Pre-Omicron.

	Early Variants	Omicron Variants
AC / mg L^{-1}		
LQ	4.4	5.3
Median	7.8	8.2
UQ	12.2	13.7
HQ / mg L^{-1}		
LQ	0.5	2.6
Median	1.7	4.0
LQ	4.5	7.5
HQ / %		
LQ	11	38
Median	27	47
UQ	45	58

References

1. Burridge HC, Fan S, Jones RL, Noakes CJ, Linden PF. Predictive and retrospective modelling of airborne infection risk using monitored carbon dioxide. *Indoor and Built Environment* 2021; **31**(5): 1363-80.
2. Manica M, Poletti P, Deandrea S, et al. Estimating SARS-CoV-2 transmission in educational settings: A retrospective cohort study. *Influenza and Other Respiratory Viruses*; **n/a**(n/a).
3. Chudasama DY, Tessier E, Flannagan J, et al. Surge in SARS-CoV-2 transmission in school-aged children and household contacts, England, August to October 2021. *Euro surveillance : bulletin Europeen sur les maladies transmissibles = European communicable disease bulletin* 2021; **26**(48).
4. Flasche S, Edmunds WJ. The role of schools and school-aged children in SARS-CoV-2 transmission. *Lancet Infect Dis* 2021; **21**(3): 298-9.
5. Evans JP, Liu SL. Challenges and Prospects in Developing Future SARS-CoV-2 Vaccines: Overcoming Original Antigenic Sin and Inducing Broadly Neutralizing Antibodies. *J Immunol* 2023; **211**(10): 1459-67.
6. Spatola M, Nziza N, Jung W, et al. Neurologic sequelae of COVID-19 are determined by immunologic imprinting from previous coronaviruses. *Brain* 2023; **146**(10): 4292-305.
7. Reynolds CJ, Pade C, Gibbons JM, et al. Immune boosting by B.1.1.529 (Omicron) depends on previous SARS-CoV-2 exposure. *Science* 2022: eabq1841.
8. James-Pemberton PH, Kohli S, Twynham J, et al. Mass-Standardised Differential Antibody Binding to a Spectrum of SARS-CoV-2 Variant Spike Proteins from Wuhan, Alpha, Beta, Gamma, Delta, Omicron BA.1, BA.4/5, BA.2.75 and BA.2.12.1 variants: Antibody Immunity Endotypes. *medRxiv* 2025: 2022.09.23.22280271.
9. Cai Y, Zhang J, Xiao T, et al. Distinct conformational states of SARS-CoV-2 spike protein. *Science* 2020; **369**(6511): 1586-92.
10. Castanares-Zapatero D, Chalon P, Kohn L, et al. Pathophysiology and mechanism of long COVID: a comprehensive review. *Annals of Medicine* 2022; **54**(1): 1473-87.
11. Davis HE, McCorkell L, Vogel JM, Topol EJ. Long COVID: major findings, mechanisms and recommendations. *Nature Reviews Microbiology* 2023; **21**(3): 133-46.
12. Turner S, Khan MA, Putrino D, Woodcock A, Kell DB, Pretorius E. Long COVID: pathophysiological factors and abnormalities of coagulation. *Trends Endocrinol Metab* 2023; **34**(6): 321-44.
13. Tas JM, Mesin L, Pasqual G, et al. Visualizing antibody affinity maturation in germinal centers. *Science* 2016; **351**(6277): 1048-54.
14. Garcia L, Woudenberg T, Rosado J, et al. Kinetics of the SARS-CoV-2 Antibody Avidity Response Following Infection and Vaccination. *Viruses* 2022; **14**(7).
15. Formolo T LM, Levy M, Kilpatrick L, Lute S, Phinney K, et al. . Determination of the NISTmAb primary structure. State-of-the-Art and Emerging Technologies for Therapeutic Monoclonal Antibody Characterization: ACS Symposium Series; 2015: 1-62.
16. McLellan JS, Chen M, Kim A, Yang Y, Graham BS, Kwong PD. Structural basis of respiratory syncytial virus neutralization by motavizumab. *Nature structural & molecular biology* 2010; **17**(2): 248-50.
17. James-Pemberton PH, Helliwell MW, Olkhov RV, et al. Mass-Standardised Quantitative Measurements of the Antibody Levels for SARS-CoV-2 beyond Correlates of Protection and Clearance *medRxiv* 2025: 2022.07.12.22277533.
18. James-Pemberton P, Łapińska U, Helliwell M, et al. Accuracy and precision analysis for a biophotonic assay of C-reactive protein. *The Analyst* 2020: 10.1039/c9an02516b.
19. Shaw AM, Hyde C, Merrick B, et al. Real-world evaluation of a novel technology for quantitative simultaneous antibody detection against multiple SARS-CoV-2 antigens in a cohort of patients presenting with COVID-19 syndrome. *Analyst* 2020.
20. James-Pemberton PH, Helliwell MW, Olkhov RV, et al. Vaccine, Booster and Natural Antibody Binding to SARS-CoV-2 Omicron (BA.1) Spike Protein and Vaccine Efficacy. *medRxiv* 2022: 2022.07.12.22277539.
21. Gurdasani D, Pagel C, McKee M, et al. Covid-19 in the UK: policy on children and schools. *BMJ (Clinical research ed)* 2022; **378**: e071234.
22. Pierce CA, Herold KC, Herold BC, et al. COVID-19 and children. *Science* 2022; **377**(6611): 1144-9.
23. WHO. Considerations for school-related public health measures in the context of COVID-19. 2020 (accessed 17th November 2022).
24. Röltgen K, Nielsen SCA, Silva O, et al. Immune imprinting, breadth of variant recognition, and germinal center response in human SARS-CoV-2 infection and vaccination. *Cell* 2022; **185**(6): 1025-40.e14.
25. Yu W, Zhong N, Li X, et al. Structure Based Affinity Maturation and Characterizing of SARS-CoV Antibody CR3022 against SARS-CoV-2 by Computational and Experimental Approaches. *Viruses* 2022; **14**(2).
26. Tang J, Grubbs G, Lee Y, et al. Antibody affinity maturation and cross-variant activity following SARS-CoV-2 mRNA vaccination: Impact of prior exposure and sex. *EBioMedicine* 2021; **74**: 103748.
27. Laidlaw BJ, Ellebedy AH. The germinal centre B cell response to SARS-CoV-2. *Nat Rev Immunol* 2022; **22**(1): 7-18.
28. Mishra AK, Mariuzza RA. Insights into the Structural Basis of Antibody Affinity Maturation from Next-Generation Sequencing. *Front Immunol* 2018; **9**: 117.
29. Victora GD, Nussenzweig MC. Germinal Centers. *Annu Rev Immunol* 2022; **40**: 413-42.
30. Tam HH, Melo MB, Kang M, et al. Sustained antigen availability during germinal center initiation enhances antibody responses to vaccination. *Proceedings of the National Academy of Sciences* 2016; **113**(43): E6639-E48.
31. McHeyzer-Williams LJ, McHeyzer-Williams MG. ANTIGEN-SPECIFIC MEMORY B CELL DEVELOPMENT. *Annual Review of Immunology* 2005; **23**(1): 487-513.

32. Ayyar BV, Arora S, Murphy C, O'Kennedy R. Affinity chromatography as a tool for antibody purification. *Methods* 2012; **56**(2): 116-29.
33. England RJ, Homer JJ, Knight LC, Ell SR. Nasal pH measurement: a reliable and repeatable parameter. *Clin Otolaryngol Allied Sci* 1999; **24**(1): 67-8.
34. COVID-19 Genomic Surveillance. 2022. https://covid19.sanger.ac.uk/lineages/raw?latitude=51.622741&longitude=-1.455710&zoom=4.708800&p_type=area&cases_type=area&xMin=2021-12-04&xMax=2022-09-24 (accessed 24/09/2022 2022).